

# Highly sensitive FET sensors for cadmium detection in one drop of human serum with a hand-held device and investigation of the sensing mechanism

Cite as: Biomicrofluidics 15, 024110 (2021); doi: 10.1063/5.0042977

Submitted: 5 January 2021 · Accepted: 30 March 2021 ·

Published Online: 12 April 2021



View Online



Export Citation



CrossMark

Shin-Li Wang,<sup>1</sup> Ching-Yen Hsieh,<sup>2</sup> Chang-Run Wu,<sup>1</sup> Jung-Chih Chen,<sup>3,4,5,a)</sup> and Yu-Lin Wang<sup>1,2,a)</sup>

## AFFILIATIONS

<sup>1</sup>Institute of Nanoengineering and Microsystems, National Tsing Hua University, Hsinchu 300, Taiwan

<sup>2</sup>Department of Power Mechanical Engineering, National Tsing Hua University, Hsinchu 300, Taiwan

<sup>3</sup>Institute of Biomedical Engineering, National Chiao Tung University, Hsinchu 300, Taiwan

<sup>4</sup>Department of Electrical and Computer Engineering, National Chiao Tung University, Hsinchu 300, Taiwan

<sup>5</sup>Department of Biological Science and Technology, National Chiao Tung University, Hsinchu 300, Taiwan

**Note:** This paper is part of the special collection, Selected Papers from the 2020 International Conference on Smart Sensors (ICSS).

**a) Authors to whom correspondence should be addressed:** [ylwang@mx.nthu.edu.tw](mailto:ylwang@mx.nthu.edu.tw) and [george@nctu.edu.tw](mailto:george@nctu.edu.tw)

## ABSTRACT

As the heavy metal contamination is becoming worse, monitoring the heavy metal content in water or human body gets more and more important. In this research, a cadmium ion-selective field effect transistor (Cd-ISFET) for rapidly detecting cadmium ions has been developed and the mechanism of the sensor is also investigated in depth. Our Cd-ISFET sensor exhibits high sensitivity beyond the ideal Nernst sensitivity, wide dynamic range, low detection limit ( $\sim 10^{-11}$  M), which is comparable with inductively coupled plasma mass spectrometry, and easy operation enabling people to detect cadmium ion by themselves. From the analysis of electrical measurement results, this Cd-ISFET is preferred to operate at the bias with the maximum transconductance of the FET to enhance the sensor signal. The AC impedance measurement is carried out to directly investigate the mechanism of an ion-selective membrane (ISM). From impedance results, the real part of the total impedance, which is the resistance, was shown to dominate the sensor signal. The potential drop across the ISM is caused by the heavy metal ion in the membrane, which is employed to the gate of the FET via an extended gate electrode. Cadmium ion detection in one drop of human serum with this sensor was demonstrated. This cost-effective and highly sensitive sensor is promising and can be used by anyone and anywhere to prevent people from cadmium poisoning.

Published under license by AIP Publishing. <https://doi.org/10.1063/5.0042977>

## I. INTRODUCTION

Heavy metal pollution has been a public concerned issue in recent years. As modern technologies are rapidly developing, heavy metal pollution is also increasing sharply. Among the list of major heavy metals, cadmium is one of the most commonly seen heavy metals existing in our daily lives.<sup>1–3</sup> Cadmium is a soft and ductile element with silver color. It is widely utilized in nickel–cadmium battery, plastic production, edible pigment, electroplating process, and paint production. People may ingest cadmium from food, air, water, herbal medicine, or cigarette.<sup>4</sup> The U.S. Environment

Protection Agency (EPA) sets the up-limit for drinking water as 0.005 mg/l (5 ppb) for cadmium. In Germany, the regulation up-limit in drinking water is the same as in the USA.<sup>5</sup> The permissible cadmium level in blood is in the range of 0.3–1.2  $\mu$ g/l (0.3–1.2 ppb =  $2.67 \times 10^{-9}$ – $1.07 \times 10^{-8}$  M), which was suggested by WHO in 1996.<sup>6</sup> Many cases were reported for cadmium pollution around the world previously.<sup>7–14</sup> Because cadmium is odorless, and it may be ingested by people without consciousness. Cadmium is difficult to be metabolized by human body and will accumulate in several organs like kidney, liver, skeleton, lung, and reproductive system.<sup>15–20</sup>

Cadmium poisoning may cause osteomalacia, itai-itai disease, and lung cancer.<sup>21</sup> Therefore, monitoring of the cadmium level daily in water or human blood is extremely critical to our health.

Currently, typical instruments used to detect cadmium are laboratory-based, including inductively coupled plasma mass spectrometry (ICP-MS), inductively coupled plasma atomic emission spectroscopy (ICP-AES), and atomic absorption spectroscopy (AAS).<sup>22–23</sup> The most sensitive instrument is the ICP-MS, which has a detection limit of  $0.5 \text{ ng/l} = 0.5 \text{ ppt}$  ( $4.5 \times 10^{-12} \text{ M}$ ) for cadmium.<sup>24</sup> However, the sample pretreatment for ICP-MS is complicated and the operation needs well trained personnel. It is time-consuming and the cost of tests is high. Potentiometry has been developed for a long time. The system of potentiometry can be small and cost-effective. The apparatus is constructed with an ion-selective electrode (ISE), a reference electrode, and a voltmeter, as shown in Fig. 1(a). The ion-selective electrode uses an ion-

selective membrane (ISM) as a filter to allow only the target ion to pass through. The principle of potentiometry is based on the Nernst equation, which originated from the equation of free energy in thermodynamics, defining the ideal Nernst sensitivity of this method.<sup>25–27</sup> Although the apparatus of the potentiometry is much smaller than the above-mentioned laboratory-based instruments, its sensitivity is not as good as those of typical laboratory-based instruments. The detection limit of potentiometry is near  $0.5 \text{ ppm}$  for cadmium,<sup>28</sup> which is higher than the cutoff value for water quality regulated by EPA. In the 1970s, Bergveld developed a model for a pH sensor using ion-sensitive field effect transistors (ISFETs). His model predicts the ideal sensitivity of the pH sensor ( $59.2 \text{ mV/pH}$ ), which is the same as the ideal Nernst sensitivity.<sup>29</sup> For most ISFET sensors reported, the sensitivity is indeed either comparable<sup>30,31</sup> or lower than the ideal Nernst sensitivity.<sup>32–35</sup> Conventional ISM-coated FETs (ISMFETs) for ion detection were

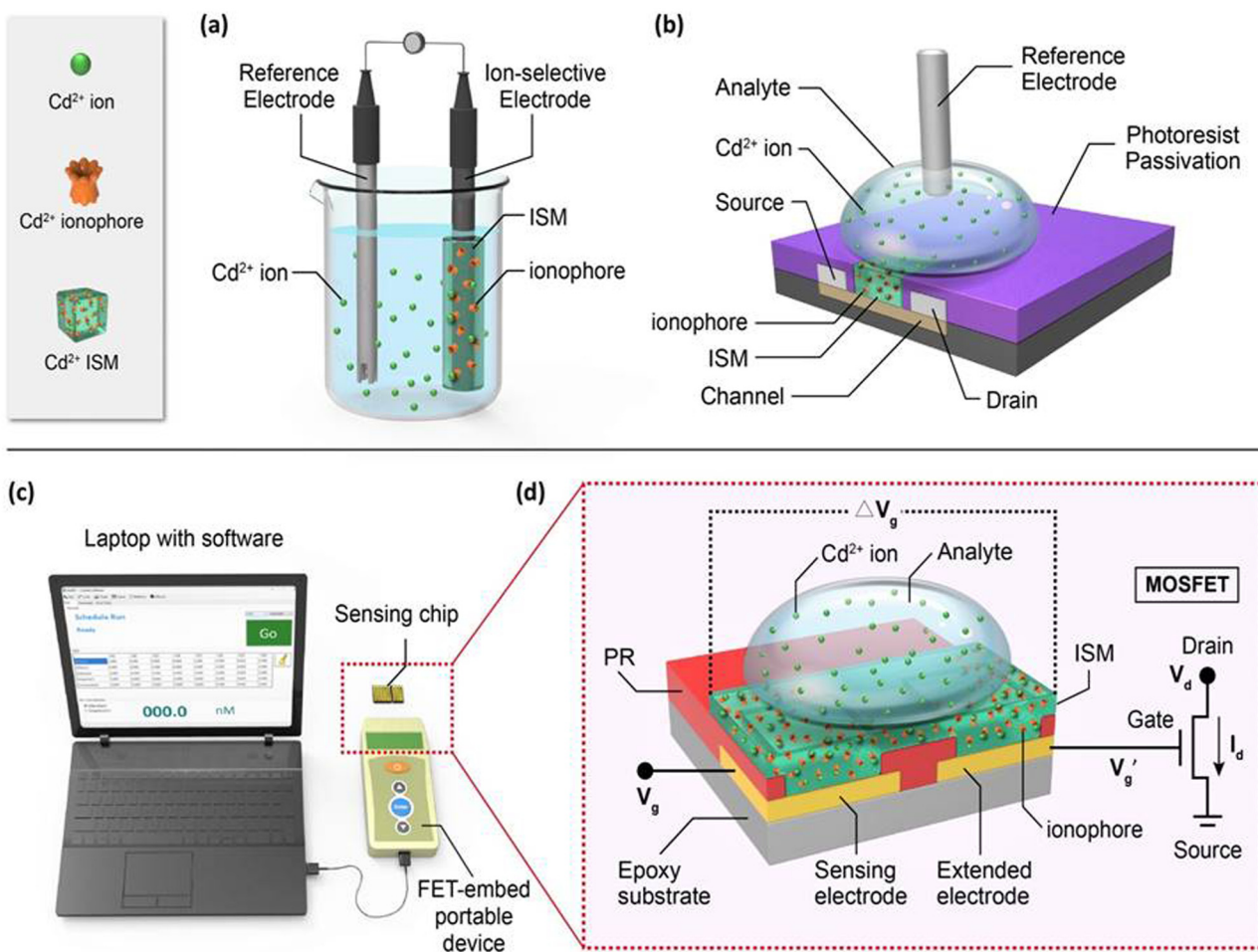


**FIG. 1.** The schematic of (a) the apparatus of the conventional potentiometry, including an ion-selective electrode, a reference electrode, and a voltmeter, (b) the conventional ion-selective membrane-coated FET sensor, (c) the portable measurement system, and (d) the ion-selective membrane conductivity-modulated FET sensor.

then reported with a lower detection limit compared to the potentiometric method.<sup>32</sup> The ISM was coated on the gate region of the FETs and a reference electrode was immersed into the test solution, as shown as in Fig. 1(b). However, the detection limit ( $3.1 \times 10^{-6}$  M) is still far beyond that of the regulation in drinking water ( $4.5 \times 10^{-8}$  M) and the sensitivity is also limited to the ideal Nernst sensitivity.<sup>32</sup> Due to the limited sensitivity, the conventional ISMFETs were regarded as one type of potentiometric device.

In this study, we have proposed a new type of ISMFET sensor, based on the change of the membrane conductivity caused by cadmium ions, resulting in the gate voltage change of the extended FET. The sensitivity of the sensor is not limited to the ideal Nernst sensitivity. A portable measurement device was also developed to measure the sensor chips. The portable measurement device is controlled by application software in a laptop, as shown in Fig. 1(c). A MOSFET was deployed in the designed circuit of the measurement device. The cadmium-selective membrane was coated across

two metal electrodes on the sensor chip. One electrode is defined as the sensing electrode and the other one is called the extended electrode. The gate voltage was applied on the sensing electrode and the extended electrode was connected to the gate of the MOSFET. The sensor chip was inserted into the measurement device through a typical PCI socket for measurement, as shown in Fig. 1(d). The cadmium-selective membrane is formed by a polyvinyl chloride (PVC) based matrix, which includes cadmium-specific ionophore, added anions, and plasticizer. As cadmium ions diffused into the membrane and were captured by the ionophore, the conductivity of the membrane changed. The change of the membrane conductivity leads to the change of the gate voltage drop in the membrane, resulting in the drain current change. Because the voltage drop of this sensor follows Ohm's law, instead of the Nernst equation, the sensitivity of this sensor is not limited and can be higher than the Nernstian one. The obtained sensitivity of the Cd-ISMFET in this study is 71 mV/decade, which is beyond

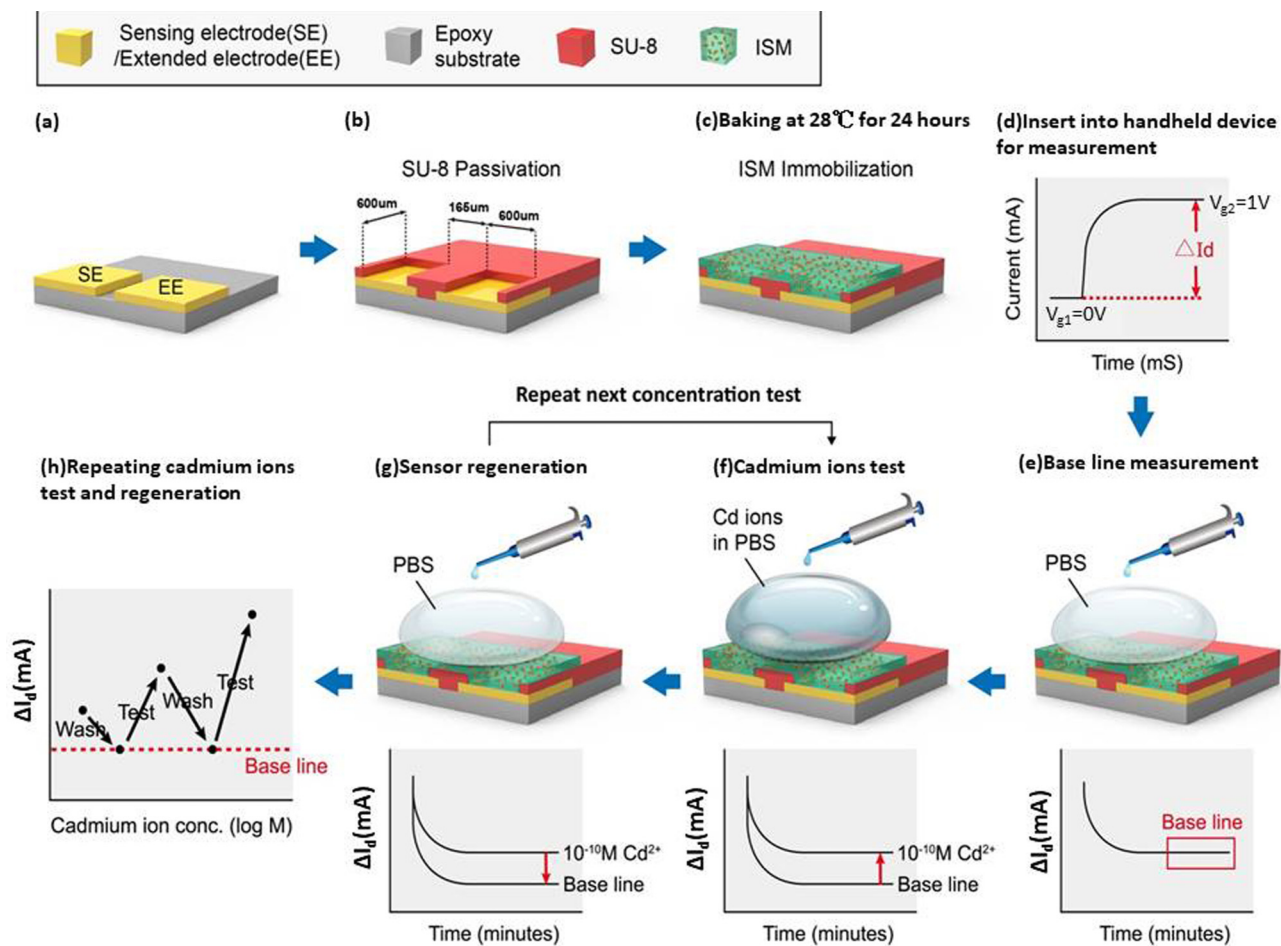


**FIG. 2.** Schematics of the experimental process. (a) Metal deposition for electrode pair. (b) Formation of the passivation layer. (c) ISM immobilization. (d) Sensor signal definition. (e) Baseline measurement in PBS. (f) Cadmium ion detection. (g) Regeneration process. (h) Multiple tests and regeneration of the cadmium ion FET sensor.

the ideal Nernst sensitivity, 29.58 mV/decade. The AC impedance measurement of the membrane-coated chip (without FETs) was also conducted to support the proposed sensing mechanism. Not only the standard buffer solutions but also human serum samples were successfully demonstrated for cadmium detection with this sensor and the device. This Cd-ISMFET sensor has shown superior high sensitivity, low detection limit, simple operation, and low cost. This sensor is affordable and convenient for anyone at anytime and anywhere for personal healthcare.

## II. EXPERIMENTAL

### A. Extended gate chip fabrication

The extended gate chip is fabricated by the following method. First, we drill a poly(methyl methacrylate) (PMMA) mold into the shape of an extended gate chip by laser cutting.

A silicon-based organic polymer, poly(dimethylsiloxane) (PDMS), is then pulled into the PMMA mold and baked at 65 °C for 2 h in the oven. PMMA mold and PDMS are separated after baking. Epoxy glue is then poured into the PDMS mold and cured at 125 and 165 °C for 90 and 60 min, respectively. This molding process was also reported previously in detail.<sup>36</sup> After peeling off the epoxy substrate from PDMS, the photolithography process is carried out, followed by metal deposition with E-gun evaporator and a lift-off process, to create an electrode pair, as shown in Fig. 2(a). Photoresist (SU-8) is coated as a passivation layer and the opening on the electrode pair is created. Each electrode pair contains a sensing electrode and an extended electrode. Gate voltage ( $V_g$ ) is applied on the sensing electrode. The extended electrode is connected to the gate terminal of the FET. The gap between the electrode pair is 165  $\mu\text{m}$  and the sensing area is  $600 \times 600 \mu\text{m}^2$  as shown in Fig. 2(b).

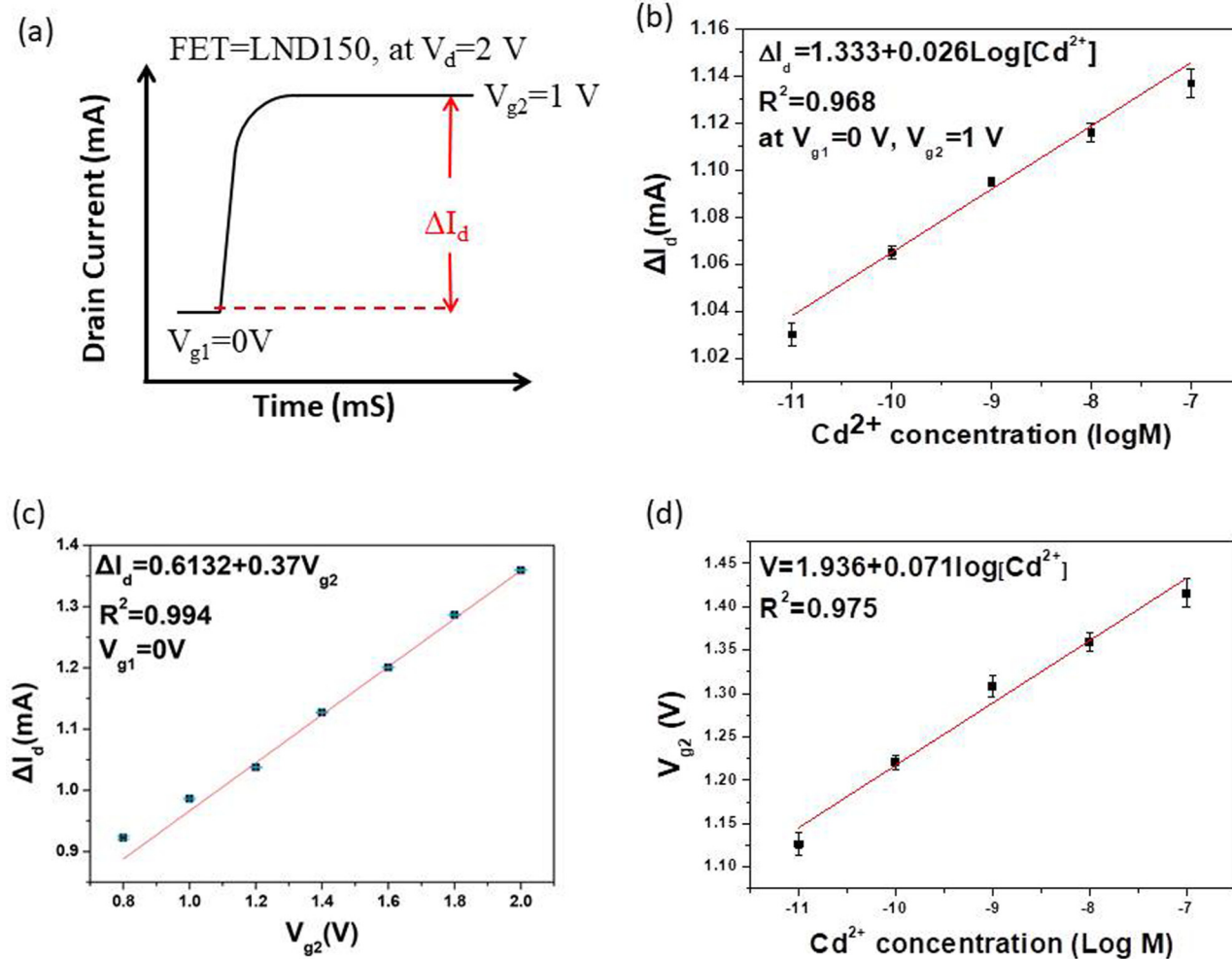


FIG. 3. (a) Definition of  $\Delta I_d$  of the FET (LND150). (b)  $\Delta I_d$  vs cadmium ion concentration. (c)  $\Delta I_d$  vs  $V_{g2}$ . (d)  $V_{g2}$  vs cadmium ion concentration.

## B. Ion-selective membrane (ISM) preparation and immobilization

The ISM is composed of four constituents: ionophore, added anion, polyvinyl chloride (PVC), and plasticizer. Cadmium ionophore I (5% by weight) is used to capture target ions. Potassium tetrakis(4-chlorophenyl)borate (0.35% by weight) is used as an added anion to adjust the conductivity of ISM. 2-nitrophenyl octyl ether (2-NOE) (63.65% by weight) acts as a plasticizer in the ISM. The amount of PVC used in this ISM fabrication is 31% by weight. These constituents are dissolved in THF. As shown in Fig. 2(c), 0.15  $\mu$ l ISM is dropped on the sensing platform and kept at 28 °C for 24 h in an oven to make sure that the solvent evaporates completely. After 24 h, the immobilization finishes and the measurements can be done. All the ingredients were purchased from Sigma.

## C. Cadmium ion samples

The cadmium ion solution is prepared by using cadmium nitrate  $[Cd(NO_3)_2]$ . The stock solution contains 0.02× phosphate-buffered saline (PBS). 2.364 mg cadmium nitrate powder is dissolved in 10 ml 0.02× PBS. This makes the stock solution concentration to be  $10^{-3}$  M cadmium ions. We then diluted the stock solution to get working concentrations from  $10^{-11}$  to  $10^{-7}$  M cadmium ions using 0.02× PBS.

The human serum is provided by a healthy person and the cadmium level of the human serum is lower than the detection limit of the laboratory-based instrument (ICP-MS). Before the measurement, we added 10  $\mu$ l cadmium ion solution into 90  $\mu$ l serum sample to prepare different cadmium ion concentrations in serum.

## D. The measurement system

In this research, we used two measurement systems. One is the laboratory-based instrument, Agilent B1500A/B1530 semiconductor analyzer, and the other one is a portable measurement system. The

portable measurement system is utilized to measure the sensor with a FET. The product numbers of the FETs are LND150 and VN10LP, respectively. LND150 is a depletion mode FET and provided by Microchip Technology. VN10LP is an enhancement mode FET and supplied by Diodes Incorporated. The prototype is connected to a laptop through a USB port and the measurement parameter can be set by software in the computer. The software was developed by us and it can set all the measurement parameters for the prototype device such as the gate bias, the duration time, the drain voltage, and the drain current. In the measurement, a steady 2 V of drain voltage ( $V_d$ ) is applied on the FET. Gate bias ( $V_g$ ) at  $V_{g1}$  is first applied on the sensing electrode for 100  $\mu$ s. Following this,  $V_{g2}$  is applied on the sensing electrode for 2 ms. Figure 2(d) elucidates the definition of  $\Delta I_d$ , which is the drain current difference between the  $V_{g1}$  and  $V_{g2}$ . After PBS is dropped on the sensing membrane, the  $\Delta I_d$  is recorded every minute until it gets steady. The sensor signal is sampled at a steady state, as shown in Fig. 2(e). The PBS droplet is then removed and the low concentration of  $Cd^{2+}$  solution is then dropped on the sensor, leading to increasing  $\Delta I_d$ , as shown in Fig. 2(f). The  $Cd^{2+}$  solution is then replaced with PBS solution and the  $\Delta I_d$  moves back to the original baseline, as shown in Fig. 2(g). The  $Cd^{2+}$  solution and the PBS are repeatedly tested, resulting in Fig. 2(h).

The AC impedance measurement results are measured by Agilent B1500A/B1530A semiconductor analyzer. In the AC impedance measurement, the sensing chip is removed from the FET. We directly probe on the sensing electrode and the extended electrode in order to the ISM impedance. The AC frequency is 1 kHz and a 3 V DC bias is applied on the sensing electrode while giving a 100 mV of AC signal.

## III. RESULTS AND DISCUSSION

Figure 3(a) defines the drain current measured for the FET, LND150, at  $V_d = 2$  V,  $V_{g1} = 0$  V, and  $V_{g2} = 1$  V, respectively. The  $\Delta I_d$

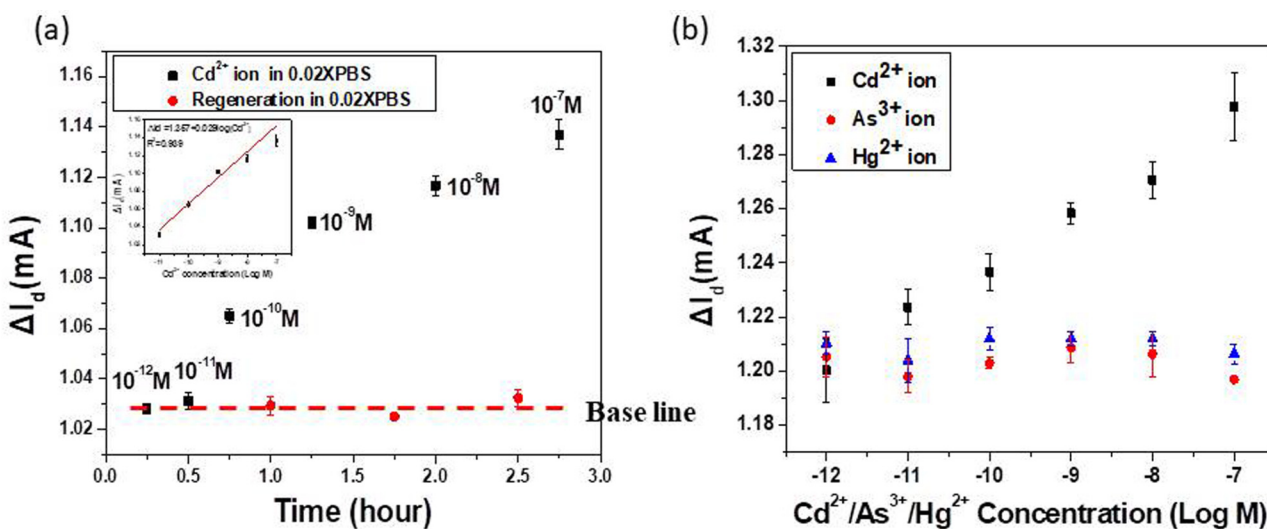


**FIG. 4.** (a) Electrical response  $\Delta I_d$  of cadmium ion-selective sensor and the regeneration. (b) Confirmation of the selectivity characteristics of Cd-ISMFET with the separated solution method.

was measured for different  $\text{Cd}^{2+}$  concentrations ranging from  $10^{-11}$  to  $10^{-7}\text{M}$ , as shown in Fig. 3(b). Figure 3(c) shows the  $\Delta I_d$  measured at different  $V_{g2}$  with only PBS and without  $\text{Cd}^{2+}$  ions in solution. By combining Figs. 3(b) and 3(c), it can lead to a

correlation between  $V_{g2}$  and  $\text{Cd}^{2+}$  concentration, as shown in Fig. 3(d). The fitting slope in Fig. 3(d) indicates the sensitivity, 71 mV/decade, which is beyond the ideal Nernst sensitivity (29.58 mV/decade).

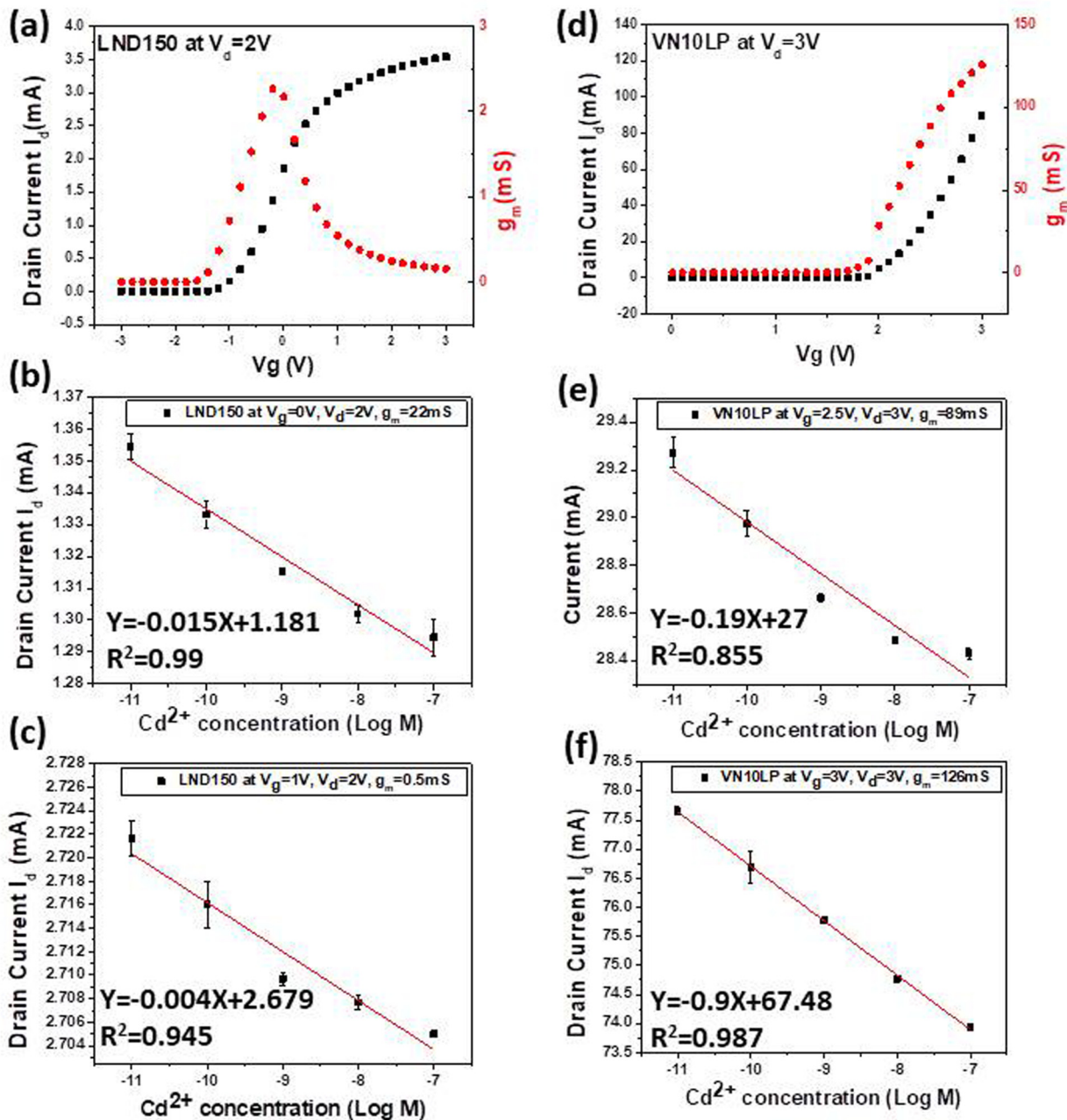


**FIG. 5.** (a) Drain current ( $I_d$ ) and transconductance ( $g_m$ ) vs gate voltage of the FET LND150 at  $V_d = 2\text{V}$ . (b) The sensor measured with the FET LND150 at  $V_d = 2\text{V}$  and  $V_g = 0\text{V}$  (c) The sensor measured with the FET LND150 at  $V_d = 2\text{V}$  and  $V_g = 1\text{V}$ . (d) Drain current ( $I_d$ ) and transconductance ( $g_m$ ) vs gate voltage of the FET VN10LP at  $V_d = 3\text{V}$ . (e) The sensor measured with FET VN10LP at  $V_d = 3\text{V}$  and  $V_g = 2.5\text{V}$ . (f) The sensor measured with FET VN10LP at  $V_d = 3\text{V}$  and  $V_g = 3\text{V}$ .

In potentiometry, the potential drop can be calculated by the Nernst equation as shown in Eq. (1),

$$E_{ISM} = c + \frac{RT}{nF} \log [A], \quad (1)$$

where  $[A]$  is the concentration of the target ion.  $F$ ,  $R$ ,  $T$ , and  $n$  are Faraday's constant, gas constant, temperature, and valence of the target ion, respectively. The valence of the cadmium ion is 2 and thus the ideal Nernst sensitivity is 29.58 mV/log[Cd<sup>2+</sup>].

Figure 4(a) shows that after a cadmium ion solution was tested, the sensor was washed and soaked in 0.02× PBS until the sensor signal ( $\Delta I_d$ ) moved back to the baseline. After the signal returns to the baseline, the next concentration of the cadmium solution was dropped on the sensor and the electrical signal was measured. This test/regeneration process was repeated through the whole dynamic range, confirming that the electrical signals have

indeed resulted from the cadmium ions captured by ionophore, but not from the baseline drifting.

The selectivity of Cd-ISFET is elucidated as shown in Fig. 4(b). The separation solution method is used to confirm the selectivity of Cd-ISMFET. The cadmium ion-selective membrane is immobilized on the sensing chip and utilized to test cadmium, arsenic, and mercury ion solution. These ions are prepared in 0.02× PBS and the concentration ranges from 10<sup>-12</sup> to 10<sup>-7</sup>M. As shown in Fig. 4(b),  $\Delta I_d$  increases when the cadmium ion concentration is increased. After the cadmium ion was tested, the regeneration procedure was performed to wash out the cadmium ions from the membrane. Arsenic ion solutions were then dropped on the sensor and tested. The electrical signal ( $\Delta I_d$ ) does not show any significant change when the arsenic ion concentration is increased. A similar electrical response was obtained when the mercury ion solutions were tested with the Cd-ISMFET. The result shows that the Cd-ISMFET has good selectivity toward

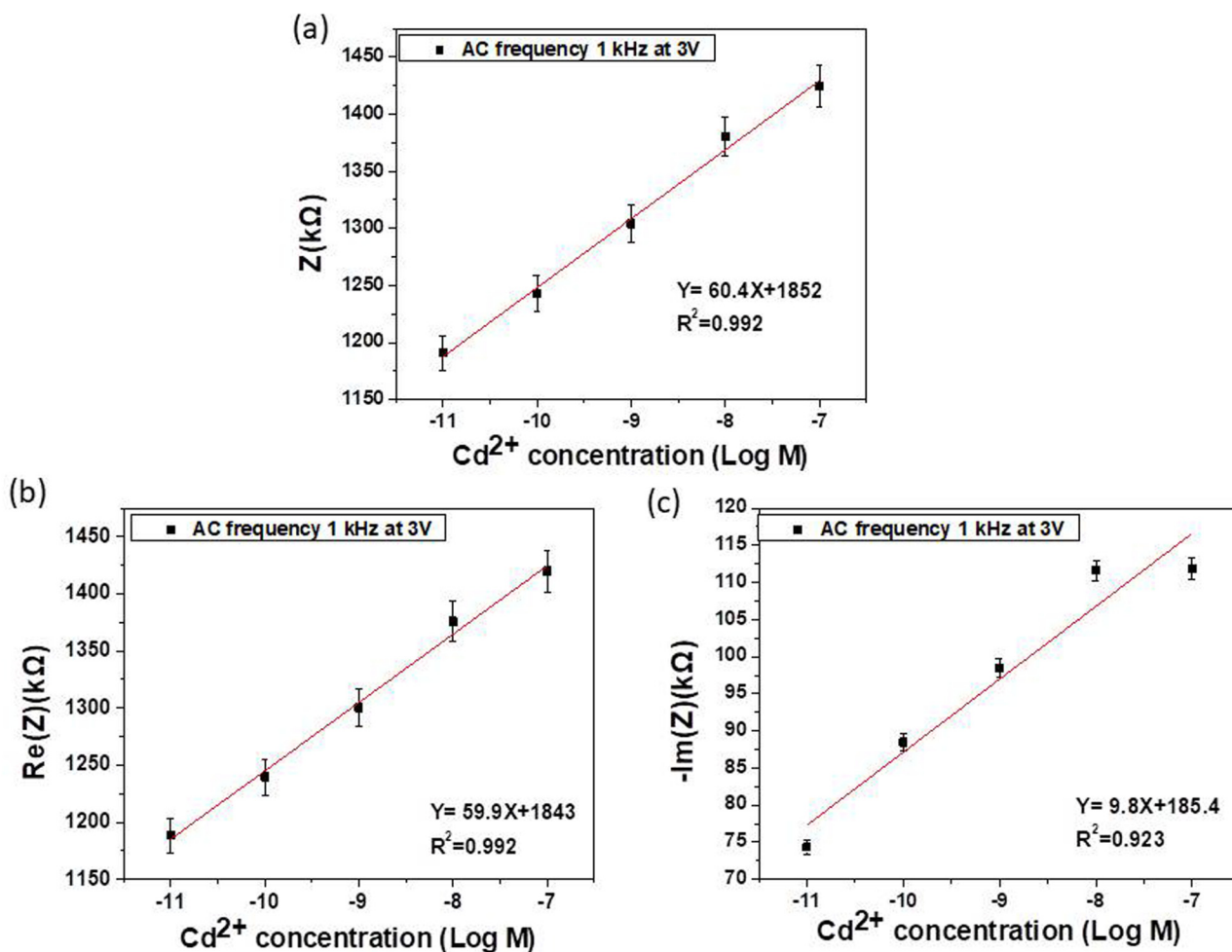


FIG. 6. (a) The total impedance (measured at 1 kHz and DC 3 V) vs cadmium ion concentration. (b) The real part and (c) the imaginary part of the total impedance varies with [Cd<sup>2+</sup>] in a decade.

arsenic and mercury ions. The selectivity is simply due to the high selectivity of the cadmium-specific ionophore in the membrane.

In order to elucidate the working principle of Cd-ISFET, two different FETs, LND150 and VN10LP, were used and compared. Figures 5(a) and 5(d) show the drain current ( $I_d$ ) and the transconductance ( $g_m$ ) vs  $V_g$  at constant  $V_d$  for LND150 and VN10LP, respectively. Obviously, the maximum  $g_m$  of LND150 is much smaller than that of VN10LP. Figures 5(b) and 5(c) show  $I_d$  vs  $[Cd^{2+}]$  of the sensor at  $V_d = 2$  V for  $V_g = 0$  V and  $V_g = 1$  V, respectively. The slope (sensitivity) at  $V_g = 0$  V, as shown in Fig. 5(b), is significantly larger than that at  $V_g = 1$  V, as shown in Fig. 5(c). The difference in sensitivity at  $V_g = 0$  and 1 V is due to the very different  $g_m$  at the two bias conditions. Figures 5(e) and 5(f) show the  $I_d$  vs  $[Cd^{2+}]$  at  $V_d = 3$  V using VN10LP for  $V_g = 2.5$  and 3 V, respectively. The slope (sensitivity) at  $V_g = 3$  V is much larger than that at  $V_g = 2.5$  V, due to the larger  $g_m$  ( $\sim 126$  mS) at  $V_g = 3$  V, compared to that ( $\sim 89$  mS) at  $V_g = 2.5$  V.

The  $I_d$ - $V_d$  characteristics of LND150 and VN10LP are provided in Figs. S1(a) and S1(b) in the [supplementary material](#), respectively. LND150 is operating in both saturation and linear regions. The chosen operation bias for this MOSFET is not only to consider the linear or saturation region but also the power consumption, which is relevant to the heat generated in the FET channel. Elevated temperature in the channel may affect the fluctuation and stability of the device. VN10LP is operating in the saturation region. In this FET, because of the much larger transconductance than that of LND150, more power consumption is acceptable due to the improved S/N ratio.

From the results shown in Fig. 5, it is obvious that the  $g_m$  plays a key role in the sensitivity of the sensor. Thus, the mechanism of the sensor can be explained as the gate voltage drop in the membrane caused by the heavy metal ions, which are captured by the ionophore, leads to the amplification of the signals through the transconductance ( $g_m$ ) of the FET.

To further confirm the sensor mechanism, the AC impedance analysis is used to investigate how cadmium ions change the membrane impedance. Agilent B1500A/B1530A semiconductor analyzer

is employed to conduct this measurement. For the impedance measurement, we directly probe on the sensing electrode and the extended electrode without connecting to the FET. Figure 6(a) depicts the total impedance vs the cadmium concentration from  $10^{-11}$  to  $10^{-7}$  M. The impedance was measured at 1 kHz and DC 3 V. As the cadmium concentration increases, the total impedance also raises. Figures 6(b) and 6(c) show the real part and the imaginary part of the total impedance vs  $[Cd^{2+}]$ , respectively. It is clear that the total impedance change has mostly resulted from the change of the real part caused by cadmium ions. This may be attributed to the reduced mobility of mobile ions caused by the complex of cadmium ions and the ionophores, leading to an increased impedance. The increased imaginary part may have resulted from the electric-double-layer capacitance change. More investigation is needed in future works. The increased total impedance successfully explains the decreased drain current of the FET shown in Figs. 5(b), 5(c), 5(e), and 5(f). The increased impedance causes more gate voltage drop in the membrane, leading to a smaller voltage applied on the extended electrode, resulting in the decreased drain current of the n-channel FET. The impedance change indicates that the voltage drop caused by heavy metal ions simply follows Ohm's law. When the membrane is connected to the FET through the extended electrode, the tiny voltage change can be amplified with the FET, based on the  $g_m$  at the operation bias. Because the sensing mechanism is based on Ohm's law, the sensitivity is therefore not limited to the ideal Nernst sensitivity. The sensitivity of this sensor depends on the composition and the fabrication process of the membrane. Compared to a complex amplification circuit, a well selected FET is much simpler and more flexible to amplify the voltage change in the membrane. This ISM-impedance modulated FET sensor is a highly integrated and simplified device but has a high sensitivity, low detection limit, and low cost. It is also easy to realize a sensor array with such kind of design for multiple target ion detection.

In this research, we employ Cd-ISFET to detect cadmium ions in human serum without any pre-treatment and compared it to cadmium ion solution in PBS buffer, as shown in Fig. 7. The cadmium ion concentration in the human serum sample has been

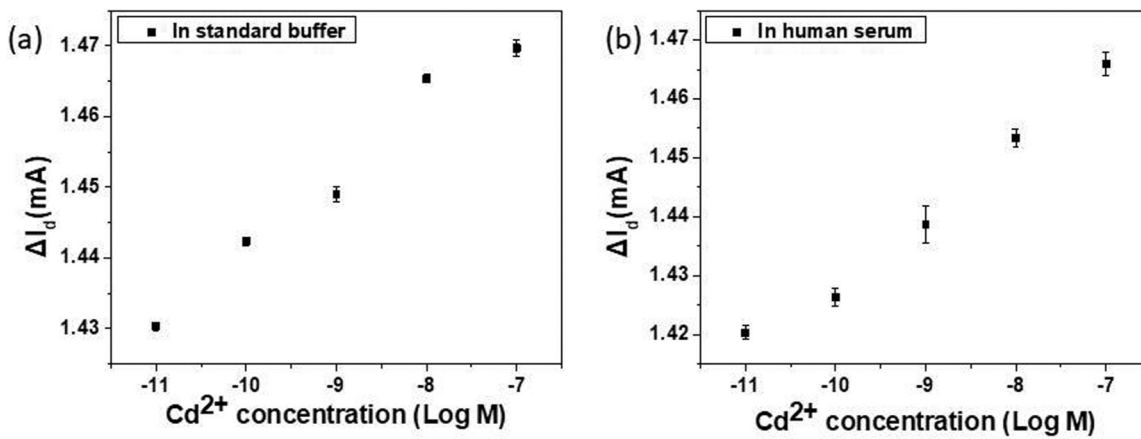


FIG. 7. Electrical characteristics for cadmium ion (a) in a 0.02× PBS buffer and (b) in human serum.

confirmed to be lower than the detection limit of the laboratory-based instruments. We spike the cadmium ions into a human serum sample with cadmium ion concentrations ranging from  $10^{-11}$  to  $10^{-7}$  M. The sensor first established a calibration curve in the standard buffer as depicted in Fig. 7(a).  $\Delta I_d$  increases as the cadmium ion concentration increases with the detection limit, as defined by the Clinical and Laboratory Standards Institute (CLSI),<sup>37,38</sup> near  $10^{-11}$  M ( $8.91 \times 10^{-12}$  M). After regeneration, the sensor detects cadmium ions in human serum as shown in Fig. 7(b). An increasing trend is observed in the calibration curve of cadmium ions with the dynamic range being  $10^{-11}$ – $10^{-7}$  M that includes the regulation limitations of the human body, which is 0.3–1.2 ppb ( $2.67 \times 10^{-9}$ – $1.07 \times 10^{-8}$  M). Proteins or other molecules in the serum may have non-specific binding on the membrane surface, but they are not able to drive into the membrane. Only the target ion can pass through the selective membrane and drive into it. From the impedance analysis, it shows that the real part of the total impedance dominates the sensor signal. The real part represents the bulk region of the membrane, not the surface region. Thus, this can explain why serum does not affect the sensor signals. We believe that the behavior of the sensor in the human serum environment is a breakthrough in the field of heavy metal ion detection and is good enough for clinic trials for cadmium toxicity testing.

#### IV. CONCLUSION

In this study, a unique extended gate structure of FET has been developed for cadmium ion detection in human serum with a portable measurement system. The sensitivity of Cd-ISFET is 71 mV/decade, which is much higher than the ideal Nernst sensitivity of 29.58 mV/decade. The dynamic range for the sensor is from  $10^{-11}$  to  $10^{-7}$  M, which includes the toxicity regulation limits for human exposure. The detection limit is 0.83 ppt. The mechanism of Cd-ISFET has been investigated by using different FET measurements and AC impedance analysis. The transconductance of the FET is the primarily effective factor for enhancing the sensor signal. The FET, VN10LP, with higher  $g_m$  at a high gate bias was employed to enlarge the sensor signal. AC impedance analysis is consistent with the FET sensors' results and indicates that the sensor signals are primarily dominated by change of the real part of total impedance, which is attributed to the change of ion mobility. The sensor successfully detects cadmium ion in human serum and its performance is not influenced by the complex composition of the serum sample. This study does not only reveal the mechanism of the sensor in depth but also demonstrates the ability and potential of our sensor to detect heavy metals at permissible toxicity levels under the influence of native microenvironments.

#### SUPPLEMENTARY MATERIAL

See the [supplementary material](#) for the FET I–V characteristic.

#### ACKNOWLEDGMENTS

This work was partially supported by research grants from the Ministry of Science & Technology (No. MOST

109-2218-E-007-017) and the National Tsing Hua University (No. 109Q2706E1).

#### DATA AVAILABILITY

The data that support the findings of this study are available from the corresponding author upon reasonable request.

#### REFERENCES

- <sup>1</sup>Agency for Toxic Substances and Disease Registry, "Toxicological profile for cadmium," p. 1.
- <sup>2</sup>K. Boonprasert, P. Kongjam, P. Limpatanachote, R. Ruengweerayut, and K. Na-Bangchang, "Urinary and blood cadmium levels in relation to types of food and water intake and smoking status in a Thai population residing in cadmium-contaminated areas in Mae Sot," *Southeast Asian J. Trop. Med. Public Health* **42**(6), 1521–1530 (2011).
- <sup>3</sup>M. Rafati Rahimzadeh, S. Kazemi, and A. A. Moghadamnia, "Cadmium toxicity and treatment: An update," *Caspian J. Intern. Med.* **8**(3), 135–145 (2017).
- <sup>4</sup>P. B. Ryan, N. Huet, and D. L. MacIntosh, "Longitudinal investigation of exposure to arsenic, cadmium, and lead in drinking water," *Environ. Health Perspect.* **108**(8), 731–735 (2000).
- <sup>5</sup>S. Völker, C. Schreiber, and T. Kistemann, "Drinking water quality in household supply infrastructure—A survey of the current situation in Germany," *Int. J. Hyg. Environ. Health* **213**(3), 204–209 (2010).
- <sup>6</sup>World Health Organization, *Trace Elements in Human Nutrition and Health* (WHO, Geneva, 1996), see [http://whqlibdoc.who.int/publications/1996/9241561734\\_eng.pdf](http://whqlibdoc.who.int/publications/1996/9241561734_eng.pdf).
- <sup>7</sup>B. Ogboko, D. Fisher, and R. Swart, "Levels of lead and cadmium in hair and saliva of school children in Ceres district, South Africa," *Afr. J. Food, Agric. Nutr. Dev.* **9**(3), 948–961 (2009).
- <sup>8</sup>M. A. Zazouli, M. Shokrzadeh, H. Izanloo, and S. Fathi, "Cadmium content in rice and its daily intake in Ghaemshahr region of Iran," *Afr. J. Biotechnol.* **7**(20), 3686–3689 (2008).
- <sup>9</sup>A. Menke, P. Muntror, E. K. Silbergeld, E. A. Platz, and E. Guallar, "Cadmium levels in urine and mortality among U.S. adults," *Environ. Health Perspect.* **117**(2), 190–196 (2009).
- <sup>10</sup>M. Berglund, K. Larsson, M. Grandér, L. Casteleyn, M. Kolossa-Gehring, G. Schwedler, A. Castaño, M. Esteban, J. Angerer, H. M. Koch, B. K. Schindler, G. Schoeters, R. Smolders, K. Exley, O. Sepai, L. Blumen, M. Horvat, L. E. Knudsen, T. A. Mørck, A. Joas, R. Joas, P. Biot, D. Aerts, K. De Cremer, I. Van Overmeire, A. Katsonouri, A. Hadjipanayis, M. Cerna, A. Krskova, J. K. Nielsen, J. F. Jensen, P. Rudnai, S. Kozepeky, C. Griffin, I. Nesbit, A. C. Gutleb, M. E. Fischer, D. Ligocka, M. Jakubowski, M. F. Reis, S. Namorado, I. R. Lupsa, A. E. Gurzau, K. Halzlova, M. Jajcay, D. Mazej, J. S. Tratnik, A. Lopez, A. Cañas, A. Lehmann, P. Crettaz, E. Den Hond, and E. Govarts, "Exposure determinants of cadmium in European mothers and their children," *Environ. Res.* **141**, 69–76 (2015).
- <sup>11</sup>M. K. Türkdoğan, F. Kilicel, K. Kara, I. Tuncer, and I. Uyan, "Heavy metals in soil, vegetables and fruits in the endemic upper gastrointestinal cancer region of Turkey," *Environ. Toxicol. Pharmacol.* **13**(3), 175–179 (2003).
- <sup>12</sup>F. Hong, T. Jin, and A. Zhang, "Risk assessment on renal dysfunction caused by co-exposure to arsenic and cadmium using benchmark dose calculation in a Chinese population," *Biometals* **17**(5), 573–580 (2004).
- <sup>13</sup>D. M. Ngo, R. L. Hough, T. T. Le, Y. Nyberg, B. M. Le, C. V. Nguyen, M. K. Nguyen, and I. Oborn, "Assessing dietary exposure to cadmium in a metal recycling community in Vietnam: Age and gender aspects," *Sci. Total Environ.* **416**, 164–171 (2012).
- <sup>14</sup>L. A. Alli, "Blood level of cadmium and lead in occupationally exposed persons in Gwagwalada, Abuja, Nigeria," *Interdiscip. Toxicol.* **8**(3), 146–150 (2015).
- <sup>15</sup>M. F. McCarty, "Zinc and multi-mineral supplementation should mitigate the pathogenic impact of cadmium exposure," *Med. Hypotheses* **79**(5), 642–648 (2012).

- <sup>16</sup>M. Trzcinka-Ochocka, M. Jakubowski, W. Szymczak, B. Janasik, and R. Brodzka, "The effects of low environmental cadmium exposure on bone density," *Environ. Res.* **110**(3), 286–293 (2010).
- <sup>17</sup>A. Engström, K. Michaësson, Y. Suwazono, A. Wolk, M. Vahter, and A. Akesson, "Long-term cadmium exposure and the association with bone mineral density and fractures in a population-based study among women," *J. Bone Miner. Res.* **26**(3), 486–495 (2011).
- <sup>18</sup>L. Järup, L. Hellström, T. Alfvén, M. D. Carlsson, A. Grubb, B. Persson, C. Pettersson, G. Spång, A. Schütz, and C. G. Elinder, "Low level exposure to cadmium and early kidney damage: The OSCAR study," *Occup. Environ. Med.* **57**(10), 668–672 (2000).
- <sup>19</sup>T. Alfvén, C. G. Elinder, M. D. Carlsson, A. Grubb, L. Hellström, B. Persson, C. Pettersson, G. Spång, A. Schütz, and L. Järup, "Low-level cadmium exposure and osteoporosis," *J. Bone Miner. Res.* **15**(8), 1579–1586 (2000).
- <sup>20</sup>A. Koyu, A. Gokcimen, F. Ozguner, D. S. Bayram, and A. Kocak, "Evaluation of the effects of cadmium on rat liver," *Mol. Cell. Biochem.* **284**(1–2), 81–85 (2006).
- <sup>21</sup>T. Inaba, E. Kobayashi, Y. Suwazono, M. Uetani, M. Oishi, H. Nakagawa, and K. Nogawa, "Estimation of cumulative cadmium intake causing itai-itai disease," *Toxicol. Lett.* **159**(2), 192–201 (2005).
- <sup>22</sup>G. Tyler and S. Jobin Yvon, ICP-OES, ICP-MS and AAS techniques compared, Technical Note 05.
- <sup>23</sup>T. Townsend, A. A. K. Miller, S. McLean, and S. Aldous, "The determination of copper, zinc, cadmium and lead in urine by high resolution ICP-MS," *J. Anal. At. Spectrom.* **13**(11), 1213–1219 (1998).
- <sup>24</sup>E. A. Group, ICP-OES and ICP-MS Detection Limit Guidance, Application Note.
- <sup>25</sup>S. Plaza, Z. Szigeti, M. Geisler, E. Martinoia, B. Aeschlimann, D. Günther, and E. Pretsch, "Potentiometric sensor for the measurement of Cd<sup>2+</sup> transport in yeast and plants," *Anal. Biochem.* **347**(1), 10–16 (2005).
- <sup>26</sup>E. Bakker and E. Pretsch, "Potentiometric sensors for trace-level analysis," *TrAC, Trends Anal. Chem.* **24**(3), 199–207 (2005).
- <sup>27</sup>V. K. Gupta, S. Chandra, and R. Mangla, "Dicyclohexano-18-crown-6 as active material in PVC matrix membrane for the fabrication of cadmium selective potentiometric sensor," *Electrochim. Acta* **47**(10), 1579–1586 (2002).
- <sup>28</sup>M. Trojanowicz, P. W. Alexander, and D. Brynn Hibbert, "Flow-injection potentiometric determination of free cadmium ions with a cadmium ion-selective electrode," *Anal. Chim. Acta* **370**(2), 267–278 (1998).
- <sup>29</sup>P. Bergveld, "Development, operation, and application of the Ion-sensitive field-effect transistor as a tool for electrophysiology," *IEEE Trans. Biomed. Eng.* **19**(5), 342–351 (1972).
- <sup>30</sup>A. Cao, M. Mescher, D. Bosma, J. H. Klootwijk, E. J. R. Sudhölder, and L. C. D. Smet, "Ionophore-containing siloprene membranes: Direct comparison between conventional Ion-selective electrodes and silicon nanowire-based field-effect transistors," *Anal. Chem.* **87**(2), 1173–1179 (2015).
- <sup>31</sup>K. Schmoltner, J. Kofler, A. Klug, and E. J. W. List-Kratochvil, "Electrolyte-gated organic field-effect transistor for selective reversible Ion detection," *Adv. Mater.* **25**(47), 6895–6899 (2013).
- <sup>32</sup>Y. Alifragis, A. Volosirakis, N. A. Chaniotakis, G. Konstantinidis, A. Adikimenakis, and A. Georgakilas, "Potassium selective chemically modified field effect transistors based on AlGaN/GaN two-dimensional electron gas heterostructures," *Biosens. Bioelectron.* **22**(12), 2796–2801 (2007).
- <sup>33</sup>S.-I. Wakida, T. Okumura, Y. Shibutani, and J. Liu, "Highly sensitive nitrate-sensing materials for ion-selective field-effect transistors for single-drop rain analysis," *Sens. Mater.* **19**, 235–247 (2007).
- <sup>34</sup>J. Liu, X. Wu, Z. Zhang, S. Wakida, and K. Higashi, "Sulfate ion-selective field effect transistors prepared by solgel technique," *Sens. Actuators, B* **66**(1), 216–218 (2000).
- <sup>35</sup>P. Li, B. Liu, D. Zhang, Y. E. Sun, and J. Liu, "Graphene field-effect transistors with tunable sensitivity for high performance Hg (II) sensing," *Appl. Phys. Lett.* **109**(15), 153101 (2016).
- <sup>36</sup>P.-C. Chen, Y.-W. Chen, I. Sarangadharan, C.-P. Hsu, C.-C. Chen, S.-C. Shieh, G.-B. Lee, and Y.-L. Wang, "Editors' choice—Field-effect transistor-based biosensors and a portable device for personal healthcare," *ECS J. Solid State Sci. Technol.* **6**(7), Q71–Q76 (2017).
- <sup>37</sup>D. Tholen, K. Linnet, M. Kondratovich, D. Armbruster, P. Garrett, R. Jones, M. H. Kroll, R. Lequin, T. Pankratz, G. A. Scassellati, H. Schimmel, and J. Tsai, "Protocols for determination of limits of detection and limits of quantitation," Approved Guidelines, 2004.
- <sup>38</sup>D. A. Armbruster and T. Pry, "Limit of blank, limit of detection and limit of quantitation," *Clin. Biochem. Rev.* **29**(Suppl. 1), S49–S52 (2008).